

EUR 5158 e

COMMISSION OF THE EUROPEAN COMMUNITIES

ON THE DETERMINATION OF THE Pu 240
IN SOLID WASTE CONTAINERS BY SPONTANEOUS
FISSION NEUTRON MEASUREMENTS.
APPLICATION TO REPROCESSING PLANT WASTE

by

R. BERG, R. SWENNEN (Eurochemic, Mol)
G. BIRKHOFF, L. BONDAR, J. LEY (Euratom, Ispra)
E. BUSCA (Euratom Safeguards Directorate, Luxembourg)

1974



MASTER

Joint Nuclear Research Centre
Ispra Establishment - Italy

DISTRIBUTION OF THIS DOCUMENT IS UNLIMITED

LEGAL NOTICE

This document was prepared under the sponsorship of the Commission of the European Communities.

Neither the Commission of the European Communities, its contractors nor any person acting on their behalf:

make any warranty or representation, express or implied, with respect to the accuracy, completeness, or usefulness of the information contained in this document, or that the use of any information, apparatus, method or process disclosed in this document may not infringe privately owned rights; or

assume any liability with respect to the use of, or for damages resulting from the use of any information, apparatus, method or process disclosed in this document.

This report is on sale at the addresses listed on cover page 4

at the price of B.Fr. 85,—

Commission of the
European Communities
D.G. XIII - C.I.D.
23, rue Aldringen
Luxembourg

September 1974

This document was reproduced on the basis of the best available copy.

EUR 5158 e

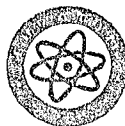
COMMISSION OF THE EUROPEAN COMMUNITIES

ON THE DETERMINATION OF THE Pu 240
IN SOLID WASTE CONTAINERS BY SPONTANEOUS
FISSION NEUTRON MEASUREMENTS.
APPLICATION TO REPROCESSING PLANT WASTE

by

R. BERG, R. SWENNEN (Eurochemic, Mol)
G. BIRKHOFF, L. BONDAR, J. LEY (Euratom, Ispra)
B. BUSCA (Euratom Safeguards Directorate, Luxembourg)

1974



Joint Nuclear Research Centre
Ispra Establishment - Italy

ABSTRACT

A non-destructive measurement system for the passive assay of plutonium in solid waste drums is described. The fission neutrons from Pu-240 spontaneous fissions are measured with a system consisting of a flexible well-type counter built up of six modular units, each containing three ^3He -counter tubes of 50 cm length, either coupled to a variable dead-time counter containing pulse amplification, -shaping and -discrimination chains for the six neutron detection units, or to a small computer (8K memory) able to do time correlation analyses of the pulse output from the detector units. The computerized part was meant to serve mainly as a reference method for the variable dead-time counter (VDC).

The system was calibrated with PuO_2 standards of known isotopic composition, distributed evenly and locally in matrix materials closely corresponding to the matrix material expected in real waste drums. Calibration extended from sub-gram quantities of plutonium to several hundred grams of plutonium.

Actual waste drums were measured, of which some contained substantial amounts of fission products giving rise to high gamma doses and others unidentified (α, n) -sources, resulting in a high neutron background. The experimental results from calibration runs are presented along with the results on the actual solid waste drums originating from the oxide production chain of the reprocessing plant. The total amount of plutonium in a drum is obtained from isotopic composition estimates.

The theoretical background and the mathematical outline of the theory is given.

<u>LIST OF CONTENTS</u>	<u>Page</u>
INTRODUCTION	5
1. DESCRIPTION OF THE INSTRUMENTATION	7
1.1 Neutron Detector Assembly for Waste Drums	7
1.2 Variable Dead-time Counter (VDC)	8
1.3 "Computerized System" for Time Correlation Analysis of Fission Neutrons	12
2. MEASUREMENTS WITH STANDARD SAMPLES IN 30 L. DRUMS	14
2.1 Determination of F_{∞}^{40}	15
2.2 Determination of the Linear Correlation Factors b_i	17
2.3 Calibration Curves	18
2.3.1 Neutron Multiplication Effects	20
2.3.2 Matrix Effects	22
3. MEASUREMENTS WITH UNKNOWN QUANTITIES OF PU IN 30 L. DRUMS	22
3.1 Results	23
3.2 Discussion of the Results	24
4. CONCLUSIONS	27
5. LIST OF REFERENCES	28
6. TABLES	29
7. FIGURES	39

INTRODUCTION

Several non-destructive techniques for the determination of Pu in solid waste based on gamma spectroscopy with a Na(I)-crystal have been described^(1,2). As solid waste drum assay for plutonium became necessary at EUROCHEMIC, the same techniques were applied. It soon became evident however, that this technique was not applicable at a reprocessing plant treating a wide variety of fuels (PWR, BWR, LWR) with a large variation in burn-up, giving plutonium with a wide range of isotopic compositions.

The next step at EUROCHEMIC was therefore the use of a high resolution Ge(Li)-detector coupled to a 1024-channel analyzer with which it was possible to scan a waste drum and:

- a) to "identify" the plutonium by estimating the probable isotopic composition,
- b) to measure the content of plutonium by using selected gamma lines of Pu-239 and
- c) to apply corrections for gamma absorption in the matrix material by evaluating lines of different energy from the same isotope.

Extensive description of a similar technique is published in ref. (3).

The results obtained by these measurements at EUROCHEMIC were routinely communicated to the EURATOM Safeguard Inspection Agency in Luxembourg.

The sometimes alarmingly high quantities of plutonium reported in these waste drums suggested to the Agency that other, independent non-destructive techniques should be applied for control.

At this point it was recognized that the gamma-spectrometry technique only would be applicable to waste drums where the plutonium

was reasonably homogeneously distributed in material where the gamma ray attenuation would not be too high (average atomic number ≤ 10).

PuO_2 might pass undetected by the gamma-spectrometric technique if sufficiently shielded.

Evidently, this problem is not so serious for passive neutron assay. On the contrary, this technique is much more sensitive to low atomic number materials. Till now gamma- and neutron assay are complementary techniques and from a safeguards point of view both should be applied, gamma-spectroscopy for establishing the isotopic composition of the material and neutron assay for the total quantity.

In the best interest of safeguards and reprocessing plant accountability, a cooperation was established between EURATOM, Luxembourg; EURATOM, Ispra and EUROCHEMIC with the aim to measure as many actual waste drums as possible with passive neutron assay techniques.

In Chapter 1 the description of the equipment involved is given. This chapter contains all relevant information about the performance of the detection- and the time correlation analysis systems. Emphasis is given to problems of the detector response under various conditions of samples and matrix materials and to the influence of high count rates on the coincidence rate for integral auto-correlation techniques (VDC - and other coincidence techniques). These problems are frequently ignored in practice, but this does not mean that they are negligible!

Chapter 2 deals with measurements with known samples, which serve for the determination of all parameters needed for the numerical analysis of the raw experimental data. An estimate of the diffi-

cult neutron self-multiplication effect is included. Measurements with reprocessing plant waste drums are reported in Chapter 3.

Conclusions from all reported experiments are listed in Chapter 4.

1. DESCRIPTION OF THE INSTRUMENTATION

A general view of the passive neutron assay equipment, which was used for measurements with 30 l waste drums is shown in Fig. 1 and a block diagram of the same is given in Fig. 2.

The various components and units of the instrumentation will be described hereafter.

1.1 Neutron Detector Assembly for Waste Drums

The neutron detector is built up of six modular units. These units are held together by two frames in such a way that they form a hexagonal well counter, in which a waste drum of maximum 34 cm diameter and 43 cm height can be placed. Top cover and bottom of the well are made of polyethylene plates of 6.2 cm thickness. Photographs of the assembly are shown in Fig. 3.

Each modular unit contains three ^3He -proportional counters of 50 cm active length, 2.5 cm diameter and 6 atm gas pressure. These counters are embedded in a moderator block of polyethylene which is clad with cadmium of 1 mm thickness. Each block is covered on the internal face of the well by a steel plate of 2 cm thickness which acts as a neutron spectrum shifter and also as a gamma-shield. On the external face a 3 cm thick polyethylene plate is mounted which serves for backscattering of fast and epithermal neutrons into the counter. Both plates together provide for raising of the neutron counting efficiency and flattening of the spectral response.

The spatial response functions $f_r(r)$ and $f_z(z)$ [$f(r, z) = f_r(r) \cdot f_z(z)$] of the counter well for fission neutrons are shown in Fig. 4. In Fig. 5 the counter response functions $f_r(R)$ and $f_z(H/2)$, respectively averaged over radius R , and height H of cylinders are plotted.

These curves serve for the evaluation of the mean counting efficiency of cylindrical drums of various sizes.

The effect of moderating matrix material on the spatial response of the counter assembly is demonstrated in Fig. 6 for drums of various diameters and 38 cm height, filled with polyethylene grains of 0.6 g/cm^3 density. These curves allow for the estimation of the effect of a strongly moderating matrix on the counting efficiency. Heavy matrix material has a much smaller influence on the counter response. For example, a fission neutron source (Cf-252) has been put in the centre of a lead cylinder of 15 cm diameter and 17 cm height (ca. 30 kg) and this gave a relative increase in the counting efficiency of about 8%.

The spectral response function normalized to the Cf-252 fission neutron energy is given in Fig. 7. A neutron decay curve is shown in Fig. 8 from which the neutron die-away time of the detector assembly has been determined as $(30.0 \pm 0.3) \mu\text{s}$. There is no measurable influence of matrix material on the die-away time. Finally, in Fig. 9 the absolute fission neutron counting efficiency $\epsilon_0(0)$ in the centre of the well is plotted as a function of discriminator settings of the VDC-unit using 1830 V detector bias voltage.

1.2 Variable Dead-Time Counter (VDC)

The instrument is described in ref. (4) and (5). A photograph of it is shown in Fig. 10 and the block diagram is included in Fig. 2. It consists of pulse amplification, -formation and -discrimination

and on the distribution of the fissile material within the matrix. From case to case there might be a variation of multiplication

chains for six neutron detector units, a pulse mixing circuit and one fast and four slow pulse counters with nominal dead-times $\tau_i = 16/\mu\text{s}$, $32/\mu\text{s}$, $64/\mu\text{s}$ and $128/\mu\text{s}$. The dead-time losses of the different pulse counters are analyzed in terms of count rates of neutrons from spontaneous fissioning nuclides, in this case essentially of Pu-240. The relationship between the fission neutron count rate and the measured count rates C_i can be established by a simple consideration of the various components of the count rates and their balance.

Let us call

C_o the count rate of the fast pulse counter and C_o^{40} and C_o^α and C_o^{bg} respectively the spontaneous fission neutron, (α, n) and background count rates of which C_o is composed, we have:

$$C_o = C_o^{40} + C_o^\alpha + C_o^{bg}$$

With analogous definitions we write the equations for the count rates C_i of the pulse counters with the dead-time τ_i as:

$$C_i = C_i^{40} + C_i^\alpha + C_i^{bg}$$

In order to determine C_o^{40} from C_o and C_i , we consider the following balance of count rates. From C_o^{40} counts per unit time a part (C_i^{40}) will trigger the counter (i) with dead time τ_i . Because the fission neutrons are emitted in groups (at the average 2.2 per event), there will be a fraction F_i^{40} of C_i^{40} correlated with the trigger pulses C_i^{40} which we call the "true coincidence count rate".

Moreover, there will be a loss of $C_i \tau_i C_o^{40}$ counts due to the dead-time τ_i of the counter (i), which we call "accidental coincidence count rate". Analogous relationships are obtained for C_o^α , C_o^{bg} and C_i^α , C_i^{bg} respectively, but F_i^α and F_i^{bg} are zero, unless neutron multiplication is taken into account. Neglecting the latter for the moment

we have:

$$C_o^{40} = C_i^{40} (1 + F_i^{40}) + C_i \tau_i C_o^{40} \quad (1. a)$$

$$C_o^\alpha = C_i^\alpha + C_i \tau_i C_o^\alpha \quad (1. b)$$

$$C_o^{bg} = C_i^{bg} + C_i \tau_i C_o^{bg} \quad (1. c)$$

$$C_o = C_i + C_i^{40} F_i^{40} + C_i \tau_i C_o \quad (2)$$

From eq. (1. a) and (2) we obtain

$$C_o^{40} = \left(C_o - \frac{C_i}{1 - C_i \tau_i} \right) \cdot \frac{1 + F_i^{40}}{F_i^{40}} \quad (3)$$

$$C_o^{40} = K_i X_i \quad (3. a)$$

with

$$K_i = \frac{1 + F_i^{40}}{F_i^{40}} \quad (4)$$

$$X_i = C_o - \frac{C_i}{1 - C_i \tau_i} = C_o + \frac{1}{\tau_i - \frac{1}{C_i}} \quad (5)$$

K_i can be determined by a calibration measurement with a small Pu-240 sample (metallic plutonium) where C_o^{40} and X_i can be measured directly. It can also be calculated from nuclear parameters (fission neutron emission multiplicity) and instrumental parameters (counting efficiency and die-away time) as shown in ref. (6). The effective dead-time τ_i is equal to the nominal dead-time (τ_{i0}) minus the discriminator paralysis time ϕ , averaged over the six counting chains. The averaged ϕ is obtained from the eq. (6).

$$\sum_{k=1}^6 \frac{C_{ok}}{1 - C_{ok} \phi_k} = \frac{C_o}{1 - C_o \phi} \quad (6)$$

where C_{ok} means the pulse rate of chain k,

ϑ_k the paralysis time of chain k , and

$C_o = \sum_{k=1}^6 C_{ok}$ the total pulse rate. Thus ϑ becomes:

$$\vartheta = \frac{\sum_{k=1}^6 \frac{C_{ok}}{1 - C_{ok}\vartheta_k} - C_o}{C_o \sum_{k=1}^6 \frac{C_{ok}}{1 - C_{ok}\vartheta_k}} \quad (7)$$

For symmetric distribution of the pulse rate, i. e. $C_{ok} = \frac{C_o}{6}$ and $\vartheta_k = \text{Const} = \vartheta_o$, we obtain $\vartheta = 1/6 \vartheta_o$.

ϑ_k depends on the pulse shape and the discrimination level, as shown in Fig. 11. In Fig. 12 are plotted the effective τ_i -values applicable for symmetric distribution of the pulses ($C_o = \frac{C_i}{6}$, $\vartheta_k = \text{const} = \vartheta_o$) as a function of the discriminator settings. These values are derived from measurements with a pure (α, n) source. Eq. (5) gives for this case

$$(X_i = 0) \tau_i = \frac{1}{C_i} - \frac{1}{C_o} \quad (8)$$

For asymmetric distributions of the pulses, formula (7) can be used for corrections.

$$\tau_i' = \tau_i + \Delta\vartheta$$

$$\Delta\vartheta = \left(\frac{1}{6} \vartheta_o - \vartheta\right)$$

Unfortunately, F_i^{40} and therefore K_i , depend on the count rate C_i itself. This is due to the fact that the higher the count rate, the more probable is the case that a spontaneous fission event occurs during the closure of the counter (i). Then a fraction of the emitted neutron population dies away before the counter may be retriggered by the

surviving fraction and accordingly F_i^{40} becomes smaller. This effect is taken into account by a linear correction term given below

$$K_i(C_i) = K_{i0}(1 + b_i C_i) \quad (9)$$

It is more convenient to include this correction term into the X_i

$$X_{i0} = X_i(1 + b_i C_i) \quad (10)$$

and to write

$$C_o^{40} = K_{i0} \cdot X_{i0} \quad (11)$$

where K_{i0} is now a constant.

The dependence of b_i on the neutron die-away time τ of the detector is shown in Fig. 13. These curves have been obtained from Monte Carlo simulation of the VDC by means of the computerized system for time correlation analysis, which is described in the following section.

The experimental determination of the b_i -values is explained in section 2.2 in connection with the calibration of the instrument.

1.3 "Computerized System" for Time Correlation Analysis of Fission Neutrons

The computerized system is described in Ref. (6). This system is generally useful for the (a) simulation and (b) measurement of the time distribution of pulses from detector-sample arrangements, and analysis of the time correlations among these pulses. In the present investigations it serves mainly as a reference method for passive neutron assay by the VDC-instrument.

The "simulation" is performed by the Monte Carlo-method. Input data are:

- i) source parameters: amount, half-life, probability distribution function of neutron emission multiplicity (p_v -distribution) of spontaneous neutron emitters (spontaneous fission or (α, n) -reactions),
- ii) multiplication parameters: probabilities for induced fission reactions in fissile isotopes of the sample and the respective neutron emission multiplicities for the various sources,
- iii) neutron detector parameters: detection probabilities and decay time of neutrons from the various sources.

Output data are:

- i) Time distribution of neutron detection pulses,
- ii) Time correlation analysis as Rossi- α -method, VDC-method and other well known pulse correlation methods.

A schematic flow diagram is shown in Fig. 14. In the case of a "measurement", the time distribution of neutron detection pulses is produced by a converter, which converts the detector pulses in their real arrival time. 8 Inputs for detector pulses are provided and each of them is labelled (1, 2, ..., 8). The data (time) are stored firstly in an 8-stage buffer memory from which they are transferred into the 8K-memory of the mini-computer (LABEN 70). The buffer memory acts as a "de-randomizer" of the time-distribution of pulses and allows for reduction of signal losses during the transfer cycles into the computer memory. A block diagram of this instrumentation is given in Fig. 15.

As a reference method for passive neutron assay techniques, we choose the well known Rossi- α -method, which does not require any correction. The Rossi- α technique allows for the separation of correlated counts from uncorrelated counts out of the time-distribution

In reality there will always be a superposition of both the self-multiplication and the matrix effects, which sometimes may add together. No clear statement is possible from

of neutron detection pulses. This is done by summing up all pulses within a time interval, Δt , which follows each individual detector pulse and subtraction of the uncorrelated counts within Δt , which are computed from the total count rate C_0 as $C_0 \Delta t$. In the picture of a coincidence counter, and this is also true for the VDC, this would mean that any detector pulse may open a coincidence gate or close all pulse counters (i) respectively. In this way there would be no need for correction either for true coincidence losses, during the time the coincidence gate was opened or the input of pulse counter was closed respectively, or for the variation of the F_i (correlated counts per pulse due to fission neutrons) with count rate C_i (linear correction factor b_i). This feature of the Rossi- α technique is therefore a possibility for testing the correction formula of the VDC method. The second weak point of the VDC is the variation of the dead times (τ_i) due to unsymmetric repartition of the detector pulses among the b pulse counting chains. Also this uncertainty is eliminated in the Rossi- α analysis, just by introducing a blank of 4 μ sec at the beginning of the time interval Δt to be analyzed.

2. MEASUREMENTS WITH STANDARD SAMPLES IN 30 L. DRUMS

The measurements with known (PuO_2) samples served for the determinations of

- i) F_{∞}^{40} = average number of neutron detector pulses correlated with the first neutron detector pulse from a Pu-240 spontaneous fission event (integral autocorrelation).
- ii) b_i = linear correction factors,
- iii) calibration curves for the VDC instrument and the computerized system.

The standard samples covered the range of Pu-240 equivalent mass (m_{eq}^{40}) between 0.09 g and 54 g.
 m_{eq}^{40} is defined according to eq. (3) as

$$m_{eq}^{40} = m^{40} \sum_k \frac{F_i^k}{F_i^{40}} \frac{1+F_i^{40}}{1+F_i^k} \frac{m_o^k}{m_o^{40}} \frac{n_o^k}{n_o^{40}} \quad (12)$$

(k includes 40)

upper index 40, k stays for Pu-240 or isotope named "k" respectively.

$m^{40,k}$ = mass of spontaneous fission isotope Pu-240 or "k" respectively.

$n_o^{40,k}$ = number of neutrons emitted per g of Pu-240 or "k" respectively.

$F_i^{40,k}$ = correlated counts per trigger of counter with dead-time τ_i by a Pu-240 neutron or "k" neutron respectively.

If $F_i^k \approx F_i^{40}$ that means: all isotopes have nearly the same fission neutron multiplicities. we can simplify eq. (12) as

$$m_{eq}^{40} = m^{40} \sum_k \frac{m_o^k}{m_o^{40}} \frac{n_o^k}{n_o^{40}} \quad (12.a)$$

This condition is nearly fulfilled for all isotopes of our interest, i. e. Pu-238, Pu-242 and U-238.

The Pu-standard samples were put into normal 30 l drums and mixed up with typical matrix materials, like gloves, cleaning papers, etc.

2.1 Determination of F_∞^{40}

F_∞^{40} is defined by the equations (13) and (14)

$$F_i^{40} = F_\infty^{40} w_i (1 - e^{-\tau_i/l}) = F_\infty^{40} \cdot \alpha_i (i = 1, 2, 3, 4) \quad w_i \leq 1 \quad (13)$$

w_i corrects for the effect of having more than one trigger (C_i^{40}) from

the same fission event. For the described equipment w_i is very close to 1;

$$C_o^{40} = X_{io} \frac{F_\infty^{40} \alpha_i + 1}{F_\infty^{40} \alpha_i} = X_{ko} \frac{F_\infty^{40} \alpha_k + 1}{F_\infty^{40} \alpha_k} \quad (k \neq i) \quad (14)$$

from which we obtain

$$F_\infty^{40} = \frac{X_{ko} - X_{io}}{X_{io} - X_{ko}} = \frac{1}{\alpha_k} \frac{1 - \frac{y_{ik}}{A_{ik}}}{y_{ik} - 1} \quad (15)$$

with $y_{ik} = \frac{io}{X_{ko}}$ and $A_{ik} = \frac{\alpha_i}{\alpha_k}$

The y_{ik} are the ratios of dead-time corrected true coincidence count rates X_{io}/X_{ko} , according to eq. (10).

The α_i (or A_{ik}) can be calculated from the known τ_i and 1 or they can be determined directly from measurements of the F_i^{40} with a small Pu-metal sample (low count rate, no (α, n) reactions) from the following relationships, derived from eq. (3):

$$F_i^{40} = \frac{C_o^{40} (1 - C_i^{40} \tau_i)}{C_i^{40}} - 1 \quad (16)$$

$$\frac{\alpha_i}{\alpha_k} = \frac{F_i^{40}}{F_k^{40}} \quad (17)$$

for $\tau_k/1 \gg 1$ we have $\alpha_k \approx 1, F_k^{40} \approx F_\infty^{40}$ and $\alpha_i \approx \frac{F_i^{40}}{F_\infty^{40}}$.

The parameter F_∞^{40} itself is defined by the following formula:

$$F_\infty^{40} \approx \frac{1}{2} \left\{ \left(\frac{\sum_{v=0}^N v^2 p_v}{\sum_{v=0}^N v p_v} \right)^{40} - 1 \right\} \quad (18)$$

where p_ν is the probability of emitting ν neutrons in a fission event of Pu^{40} .

In principle the measurement of F_∞^{40} allows the matrix effect, i. e. the influence of the matrix material on the detection efficiency ϵ , to which F_∞^{40} is directly proportional, to be estimated. However, the F_∞^{40} determined by the y_{ik} and A_{ik} measurements according to formula (15) is very sensitive to the uncertainties of those quantities δy_{ik} , δA_{ik} respectively.

$$\delta F_\infty^{40} = \frac{1}{\alpha_k} \left\{ \frac{\frac{1}{A_{ik}} - 1}{(1-y_{ik})^2} \delta y_{ik} + \frac{y_{ik}}{A_{ik}^2 (1-y_{ik})} \delta A_{ik} \right\} \quad (19)$$

The behaviour of this function in the range $1 \geq \epsilon \geq 0.03$ is shown in Fig. 16.

Generally, the A_{ik} can be determined to about $\delta A_{ik} = \pm 0.01$. The uncertainty of the y_{ik} may also be about $\delta y_{ik} = \pm 0.01$ for not too high count rates (C_i). Under such conditions the relative uncertainty of the actual $F_\infty^{40} = 0.066$ (for $\epsilon = 0.062$) amounts to about

$$\frac{\delta F_\infty^{40}}{F_\infty^{40}} = \pm 17\%$$

The precision of the F_∞^{40} -measurement can be improved significantly, by raising the detector efficiency ϵ . In Table I the measured α_i , A_i , y_i and F_∞^{40} values are summarized.

2.2 Determination of the Linear Correction Factors b_i

The linear correction factor b_i takes into account the variation of the F_i^{40} with the count rate C_i as defined by eq. (9) and eq. (10), b_i is determined by the relationship:

$$\frac{(y_{ik})_{C_i}}{(y_{ik})_0} = \frac{1 + b_i C_i}{1 + b_k C_k} \quad (20)$$

$$b_i = \frac{1}{C_i} \left\{ \frac{(y_{ik})_{C_i}}{(y_{ik})_0} (1 + b_k C_k) - 1 \right\} \quad (21)$$

where $(y_{ik})_{C_i}$ means $\frac{X_i}{X_k}$ for C_i

and $(y_{ik})_0$ means $\frac{X_i}{X_k}$ extrapolated for $C_i = 0$. (see Fig. 17)

For $k = 1$, we have $b_k C_k < b_i C_i \ll 1$ and b_k does not need to be known very exactly, for the determination of the b_i ($i = 2, 3, 4$). In fact b_k was determined directly from X_k -measurements with a small Pu-metal sample as a function of the count rate C_k , which was varied by adding (α, n) source-neutrons. These experimental results agreed very well with a Monte Carlo-calculation by means of the computerized system.

The experimental b_i -values are derived from the plots X_i/X_1 as functions of C_i of Fig. 17.

A summary of the experimental and Monte Carlo-results is given in Table 2.

2.3 Calibration Curves

Calibration curves for VDC- and Rossi- α -techniques are given in Fig. 18.

Least squares fits to polynomials showed that the best fitting functions are of the type

$$m_{eq}^{40} = a_{0i} + a_{1i} X_i + a_{2i} X_i^2 \quad \text{for VDC technique and}$$

$$m_{eq}^{40} = a_{0\alpha} + a_{1\alpha} X_\alpha + a_{2\alpha} X_\alpha^2 \quad \text{for Rossi-}\alpha\text{-technique.}$$

All curves from VDC-techniques are essentially of the same shape. This is more directly demonstrated by the best-fitting parameters, for which the following equations must hold:

$$\begin{aligned} a_{oi} &= a_{ok} & (22) \\ a_{2k} &= a_{2i} \left(\frac{a_{1k}}{a_{1i}} \right)^2 \end{aligned}$$

Equivalence between VDC and Rossi- α -techniques is checked by analogous conditions:

$$\begin{aligned} a_{oi} &= a_{o\alpha} & (23) \\ a_{2\alpha} &= a_{2i} \left(\frac{a_{1\alpha}}{a_{1i}} \right)^2 \end{aligned}$$

The experimental results confirm the conditions (22) fairly well but not as well for the conditions (23). This indicates a certain systematic discrepancy between VDC and Rossi- α analysis. In principle, the Rossi- α -technique should be more exact than VDC owing to the uncertainties of the linear correction factor (b_1) and the effective dead-time (τ_1) of the VDC technique. These uncertainties cause systematic errors for high count rates, i.e. large Pu-240 amounts, which are affecting the coefficients a_{2i} of the quadratic correction terms of the calibration curves. These terms take account of various non-linear phenomena which are mainly due to the neutron multiplication and slowing down properties of the standard samples. The slowing down properties are essentially determined only by the hydrogenous matrix materials. As the matrix was always the same for all standard samples, we may conclude that the quadratic correction term of the calibration curve mainly describes the neutron multiplication effect.

2.3.1 Neutron Multiplication Effects

Neutron multiplication by induced fission processes, in Pu-239 and Pu-241 mainly, changes the neutron emission multiplicity. Both the spontaneous fission and the (α, n) neutrons are contributing to this effect. An exact treatment of this problem is very difficult and it is unresolvable for unknown samples. Nevertheless, a working hypothesis for estimating the magnitude of this effect can be established. In the case of PuO_2 standard samples, the ratio of spontaneous fission to (α, n) neutron emission and therefore $X_i/C_{os} = r_i$ is nearly constant. The production of induced fission neutrons,

$$P_s = (\bar{\Phi} \cdot \nu \Sigma_f \cdot V)_s$$

should be proportional to the square of the Pu-mass, because both the mean neutron flux $\bar{\Phi}$ and the mean induced fission cross section $\Sigma_f V$ are proportional to the Pu-mass (V means the volume of the sample).

In the case of Pu-waste, the assumption about the constant spontaneous fission to (α, n) neutron emission ratio cannot be maintained. but we may account for this by a correction factor on the neutron flux. If we assume that the neutron flux $\bar{\Phi}$ is proportional to the count rate C_o , this flux correction factor is equal to the ratio of the count rate C_o of the unknown sample to the count rate C_{os} of the standard sample. The production of induced fission neutrons in the unknown sample can be written therefore as

$$P = P_s \cdot \frac{C_o}{C_{os}} \approx km^2 \frac{C_o}{C_{os}} = km^2 r_i \frac{C_o}{X_i} \quad (24)$$

If we further assume that the coincidence count rate, ΔX_i , due to induced fission events, is proportional to P , we obtain

$$\Delta X_i = \Delta X_{is} \frac{C_o}{C_{os}} \approx p_{2i} \cdot m^2 \frac{C_o}{C_{os}} = p_{2i} m^2 r_i \frac{C_o}{X_i} \quad (25)$$

where $\Delta X_{is} = p_{2i} m^2$ is the coincidence count rate due to induced fissions in the standard sample.

The relationship between p_{1i} and the best fitting parameters of the calibration curves a_{1i} and a_{2i} is obtained from the equations ($a_{oi} \approx 0$, $p_{oi} \approx 0$ neglected)

$$m = a_{1i} X_i + a_{2i} X_i^2 \quad (26)$$

$$X_i = p_{1i} m + p_{2i} m^2 \quad (27)$$

or

$$m = \frac{1}{2} \frac{p_{1i}}{p_{2i}} \left(\sqrt{1 + \frac{4p_{2i}}{p_{1i}^2} X_i} - 1 \right) \quad (28)$$

$$\text{For } \frac{4p_{2i}}{p_{1i}^2} X_i = 4p_{2i} \cdot a_{1i}^2 X_i \ll 1 \quad (p_{1i} = \frac{1}{a_{1i}})$$

the root expression of equation (28) can be expanded in a Taylor series ignoring the third order term. Comparison of coefficients gives

$$p_{2i} \approx - \frac{a_{2i}}{a_{1i}^3}$$

In all assumptions mentioned above, the correction for the neutron multiplication effect of unknown samples, i. e. the difference relative to standard samples is equal to

$$\Delta m_{eq}^{40} = a_{2i} X_i^2 \left(1 - \frac{C_o}{C_{os}}\right) = a_{2i} X_i^2 \left(1 - r_i \frac{C_o}{X_i}\right) \quad (29)$$

The various parameters for the calculation of ΔX_i and Δm_{eq}^{40} are summarized in Table 3.

In reality, the neutron multiplication effect is much more complicated. It depends strongly on the moderating properties of the matrix

0.19 0.01 0.12 0.05 0.13 0.72 0.04 0.46 0.11 0.01 0.02 0.10 0.09 0.13 0.09 0.05 0.24 0.06 0.05 0.24 0.04 0.04 0.004

and on the distribution of the fissile material within the matrix. From case to case there might be a variation of multiplication effect by order of magnitude.

2.3.2 Matrix Effects

The influence of a polyethylene matrix which is one of the strongest moderating media, on the counting efficiency of the detector assembly, is shown in Fig. 6, especially by the curve $\epsilon_0(R)/\epsilon_0(0) f.(R)$.

From this curve one can estimate the maximum possible variation of the counting efficiency for a given net weight of the waste drum, just assuming that all the matrix material in the waste is composed of highly moderating materials. If a variation of the counting efficiency within $\pm 10\%$ (corresponding to $\pm 20\%$ variation of the calibration curves) is considered as tolerable, the net weight of the waste drum should not exceed 3 kg. On the other hand, weakly moderating matrix does not perturb so much the counting efficiency. A multiple of the 3 kg limit can be allowed for high Z materials as matrix, like Fe, Cu, Pb, etc. without exceeding the $\pm 10\%$ limit for the variation of the counting efficiency. Therefore, it is highly desirable to measure the counting efficiency directly. A possibility of such a measurement is explained in the section 2.1. Owing to the dependence of the precision of this method on the counting efficiency itself, as shown in Fig. 16, this method is restricted to high efficiency detectors. Moreover, owing to the increase of systematic errors of the coincidence count ratios (X_i/X_k) with count rate C_0 , this method is also limited to low count rates of about smaller than $5 \cdot 10^3$ cps. These limitations of the method are anyhow adapted to the problem, because waste materials contain generally small amounts of Pu.

3. MEASUREMENTS WITH UNKNOWN QUANTITIES OF Pu IN 30 l WASTE DRUMS

After calibration of the instruments, 134 measurements with waste

drums have been performed during a period of about 3 months. No calibrations of the instruments were done during this period. As far as the VDC instrument is concerned, no breakdown has been observed. On the other hand, an electronic defect of the "fast data acquisition unit" (de-randomizer) was discovered after 1 month operating time. This defect caused systematic errors in the analysis and it was detected because of discrepancies between the VDC and Rossi- α (computer) results. For this reason the "de-randomizer" had to be repaired and the 18 most interesting waste drums were re-measured. These measurements finally serve for comparison between the Rossi- α method (reference method) and the VDC method. It is clear that this comparison gives a direct answer about the validity of the VDC analysis method.

3.1 Results

The results of the analysis of all 134 measurements are summarized in Tables 4 and 5.

In Table 4 the results of 18 measurements for comparison between VDC and Rossi- α analysis are given. Table 5 represents the VDC results for all measurements which have been made. The data are presented in the same sequence as they have been measured over a 3 months period. Some of the waste drums have been measured several times, for example drum code E 281-2 has been measured 4 times during 3 months and no drift of the results is observed. The quoted error limits are the sum of three sources of error:

- i) counting statistics $\Delta_1 X_i$
- ii) uncertainty and variation of the effective counter dead times $\Delta_2 X_i$
- iii) uncertainty of the linear correction factor b_i .

$\Delta_1 X_i$ is calculated from the standard error of the count rate C_0 , which is equal to $\sqrt{C_0}$ and from the statistical error of the dead times losses $(C_0 - C_1)$ which is equal to $\sqrt{C_0 - C_1}$. With these standard

errors we obtain:

$$\Delta_1 X_i = \pm \left\{ \frac{1+C_i b_i}{\sqrt{t}} \left(\sqrt{C_o} - \frac{\sqrt{C_o - C_i}}{1-C_i \tau_i} \right) \right\} \quad (30)$$

where t means the total counting time,

$\Delta_2 X_i$ and $\Delta_3 X_i$ are obtained from error propagation of $\Delta \tau_i$ and Δb_i respectively.

$$\Delta_2 X_i = \pm \left(\frac{C_i}{1-C_i \tau_i} \right) (1 + C_i b_i) \Delta \tau_i \quad (31)$$

$$\Delta_3 X_i = \pm \frac{C_i}{1+C_i b_i} X_i \Delta b_i \quad (32)$$

$$\Delta X_i = \pm (|\Delta_1 X_i| + |\Delta_2 X_i| + |\Delta_3 X_i|) \quad (33)$$

From ΔX_i we calculate the uncertainty of the Pu eq. mass as

$$\Delta m = \pm (a_{1i} \Delta X_i + 2a_{2i} X_i \Delta X_i) \quad (34)$$

where a_{1i} and a_{2i} are the parameters of a best fitting parabola to the calibration curves.

No corrections have been applied for neutron multiplication- and matrix effects. The methods for estimating these effects, (as explained in sections 2.3.1 and 2.3.2) are not sufficiently accurate.

3.2 Discussion of the Results

The important question concerning the validity of the VDC concept for time correlation analysis has been rigorously tested by the comparison with a standard method, the Rossi- α technique. The time correlation analysis of the waste measurements also is an extremely hard testing in so far as the neutron emission rate of some of the waste drums is very high and in addition the ratio of correlated to uncorrelated counts is very low. For instance the waste drum E 250 gave a count rate of 2.2×10^4 cps and the ratio of correlated

to uncorrelated counts was about 80% smaller as compared to the PuO_2 standard samples.

The results of the comparison between the VDC and Rossi- α analysis, as given in Table 3, show that both methods are fully equivalent, because there is a complete agreement of all results within the error limits. Generally, the error limits of the VDC analysis are decreasing with increasing dead-time τ_1 . There is also a certain systematic "drifting" of the values for the Pu equivalent mass which is growing up with τ_1 . This effect is due to the systematic variation of the effective dead-time τ_1 , for unsymmetric repartition of the count rate C_0 among the six pulses counting chains, as explained in section 1.2. This variation $\Delta\theta$ is always negative and tends to underestimate the coincidence count rate X_1 by

$$\Delta X_1 = - C_1 C_0 \Delta\theta.$$

This error is generally increasing with the count rate C_0 and relatively decreasing with increasing τ .

The second important point is the reproducibility of the results and also this point has been checked rigorously for the VDC. The results of VDC measurements in Table 4 demonstrate that there is full agreement within the quoted error limits for all measurements during a 3 months' operation without recalibration of the instruments without rejecting any data of measurements which were routinely made and processed.

The third point of main interest concerning the matrix effect, can not be considered as resolved completely. From all investigations there is however, a general statement possible about this problem. This allows waste drums to be classified by their measured net weight into two categories. One for which the maximum systematic error limits can be assigned and another category where the error limits might be exceeded. This simply means that a maximum possible error can be deduced from the net weight of the drum, assuming that all the matrix material is composed of highly neutron moderating material like polyethylene, which makes the maximum perturbation of the calibration

curves. In the plot of the variation of the detector response as a function of quantity of polyethylene as matrix material in Fig. 6 we see an oscillation of this function from positive to zero and finally to negative perturbations, with increasing amount of matrix material. This behaviour is a characteristic of the detection assembly. It is quite reasonable to set the tolerance level of the matrix effect equal to the maximum positive perturbation, which is about 10% and to set the maximum net weight limit at the negative perturbation of -10%, which is equal to about 3 kg. The maximum bias can be calculated from the actual distribution of the net weight between 0 and 3 kg just by taking a weighted average over the perturbation functions in Fig. 6. Moreover, it must be kept in mind, that a variation of the detection probability (response) by $\pm 10\%$ results in about $\pm 20\%$ perturbation of the coincidence count rate, i. e. of the calibration factor.

The next step would be to determine the matrix perturbation of the waste drums which exceed the 3 kg limit. For this purpose we consider the determination of F_{∞} according to eq. (15). Here we need a precision for F_{∞} at least within $\pm 10\%$. This could be obtained by a detection head with at least 0.2 counting efficiency as shown in section 2.1 and Fig. 26. This possibility will be investigated in detail. The present detection head with 0.062 counting efficiency is not suitable for the required precision of F_{∞} .

A difficult point is the neutron multiplication effect; from what has been explained in section 2.3.1, it might be important for waste drums with large Pu content and high neutron flux. An extreme example for this problem is the drum E 250 (50 g Pu-240 - equivalent and 2.2×10^4 cps).

The correction for self-multiplication according to eq. (29) amounts to -35% for VDC results and -20% for Rossi- α results. These figures are however, very rough estimates.



In reality there will always be a superposition of both the self-multiplication and the matrix effects, which sometimes may add up or compensate each other. No clear statement is possible from the experimental data.

4. CONCLUSIONS

The reported measurements of the Pu-240 content in waste drums from the EUROCHEMIC reprocessing plant represent a severe test on the usefulness of passive neutron assay techniques. The analysis of the experimental data allows for the definitions of the capabilities and limitations of the instruments involved in this exercise.

1. The VDC method is equivalent to the Rossi- α method for all investigated waste drums, corresponding to a maximum neutron count rate of 2.2×10^4 cps.
2. The VDC instrument has proved the highest degree of stability and operational reliability.
3. The matrix effect can be estimated from the net weight of the waste drums. Detailed investigations are required for the evaluation of the corrections from experimental data. The procedure is explained in section 2.3.2 of this paper.
4. The neutron multiplication effect is a severe source of error for drums with large amount of Pu and high neutron flux.
5. The detection limit of the VDC method is about 1 mg Pu-240 equivalent for a 15' measuring time and low background of epithermal and fast neutrons.
6. For a maximum of 3 kg of any kind of matrix material and a maximum of about 10^4 cps the accuracy of the measured Pu-240 equivalent mass should stay within $\pm 20\%$ relative error limits.

For the drums measured in this work, EUROCHEMIC had a good estimate of their isotopic composition, both from administrative control (drum origin, time of filling the drum, mass spectrometric data on the material at the exit points) and from high resolution gamma-spectrometric measurements on drums and standards (see ref. (3)).

Thus, the measurements performed in this work can be used with confidence for accountability and safeguards purposes, since the total plutonium content is obtained by multiplying the found Pu-240 content with the appropriate factor.

5. LIST OF REFERENCES

- (1) COLE, H. A.; "An Automatic Drum Scanning System for the Measurement of Plutonium in Waste." Nucl. Inst. Meth., 65 (1968) 45
- (2) FONTAINE, A., BAUDE, L. et al.; "La Détection du Plutonium dans des Futs de Déchets Solides Compactables." CEA-R-3725
- (3) CLINE, S. E.; "A Relatively Simple and Precise Technique for the Assay of Plutonium Waste." ANCR-1055 (1972)
- (4) BIRKHOFF, G., BONDAR, L., COPPO, N., LEY, J., NOTEA, A.; "Application of Correlation Methods for Non-Destructive Measurements of Spontaneous Fission Isotopes in Mixed Fuels." IAEA-SM-133/22 (1970)
- (5) BIRKHOFF, G., BONDAR, L., COPPO, N.; "Variable Dead-Time Neutron Counter for Tamper-Resistant Measurements of Spontaneous Fission Neutrons." EUR-4801 c (1972)

- (6) BIRKHOFF, G., BONDAR, L.; "Computerized System for the Application of Fission Neutron Correlation Techniques in Nuclear Safeguards." EUR-4799 e (1972)

6. TABLES

TABLE 1 - Experimental Data for Evaluation of F_{∞}^* (see eq. (15))
from Measurements with PuO_2 -samples.

i	α_i	A_{i1}	$y_{i1} = \frac{a_{i1}}{a_{1i}}$	F_{∞}
1	0.373 ± 0.002	1.000	1.000	-
2	0.615 ± 0.002	1.649 ± 0.010	1.614 ± 0.01	0.088 ± 0.050
3	0.862 ± 0.003	2.311 ± 0.015	2.214 ± 0.01	0.093 ± 0.030
4	0.981 ± 0.004	2.630 ± 0.018	2.523 ± 0.01	0.072 ± 0.018

* from measurements with Pu-metal standard $F_{\infty} = 0.066 \pm 0.002$

TABLE 2 - Calculated and Experimental Linear Correction Factors (b_i)

i	b_i (μsec)	
	calculated value	experimental value
1	8.0 ± 1.6	8.0 ± 3
2	19.0 ± 1.7	16.0 ± 3
3	32.0 ± 2.0	28.0 ± 3
4	42.0 ± 2.0	38.0 ± 3

TABLE 3 - Parameters for Estimation of the Neutron Multipli-
cation Effect According to eq. (25), (29).

i	a_{1i} [g sec]	a_{2i} [g sec ²]	P_{2i} [g ⁻² sec ⁻¹]	r_i
1	0.6056	- 0.00088	0.00396	0.0155
2	0.3752	- 0.00034	0.00647	0.0251
3	0.2736	- 0.00018	0.0088	0.0342
4	0.2400	- 0.00013	0.0094	0.0387
Rossi- α	0.3324	- 0.00015	0.00408	0.0255

TABLE 4 - COMPARISON OF VDC - AND ROSSI- α -TECHNIQUES

Run No.	Sample Code	C_0 (cps)	Pu-240 equivalent mass (g)				Rossi- α Results
			ξ_1	VDC-Results for		ξ_4	
			ξ_2	ξ_3			
1	E 250	22,100.5	45.6 \pm 18.5	50.4 \pm 12.8	50.8 \pm 9.8	53.8 \pm 3.3	51.1 \pm 5.9
2	E 272-2	22,401.8	45.2 \pm 19.0	51.9 \pm 13.2	52.4 \pm 10.	45.9 \pm 8.4	56.5 \pm 4.1
3	E 243-3	12,944.2	16.8 \pm 6.3	18.9 \pm 4.5	20.3 \pm 3.4	21.6 \pm 3.0	18.0 \pm 2.2
4	E 281-2	8,720.3	35.9 \pm 3.5	34.3 \pm 2.5	34.9 \pm 2.0	36.8 \pm 1.8	36.9 \pm 1.2
5	E 244-3	1,959.4	9.01 \pm 0.34	9.11 \pm 0.26	9.14 \pm 0.23	9.02 \pm 0.23	9.19 \pm 0.23
6	E 255-2	2,626.4	6.69 \pm 0.46	6.86 \pm 0.35	6.92 \pm 0.30	6.85 \pm 0.30	6.68 \pm 0.32
7	E 245	4,877.9	16.3 \pm 1.26	16.7 \pm 0.93	16.7 \pm 0.72	17.0 \pm 0.71	17.0 \pm 0.64
8	E 283-2	3,143.0	7.10 \pm 0.60	6.71 \pm 0.44	7.32 \pm 0.38	7.21 \pm 0.37	7.07 \pm 0.39
9	E 137	949.0	4.89 \pm 0.15	4.96 \pm 0.12	4.81 \pm 0.10	4.90 \pm 0.11	4.87 \pm 0.11
10	E 243-2	3,425.9	5.70 \pm 0.66	6.20 \pm 0.49	6.25 \pm 0.41	5.49 \pm 0.40	5.93 \pm 0.43
11	E 277-2	4,374.6	8.94 \pm 0.99	9.19 \pm 0.72	9.25 \pm 0.60	9.36 \pm 0.57	9.95 \pm 0.57
12	E 183-2	6,676.2	28.2 \pm 2.2	27.9 \pm 1.6	29.3 \pm 1.3	27.9 \pm 1.2	30.1 \pm 0.90
13	E 271-2	1,399.3	8.13 \pm 0.23	8.16 \pm 0.18	8.40 \pm 0.16	8.59 \pm 0.17	8.72 \pm 0.17
14	E 208-1	1,819.1	9.47 \pm 0.318	9.70 \pm 0.25	9.90 \pm 0.22	9.98 \pm 0.22	9.81 \pm 0.22
15	E 269-1	4,923.0	29.0 \pm 1.44	29.9 \pm 1.01	29.8 \pm 0.91	29.6 \pm 0.82	30.3 \pm 0.62
16	E 174	1,437.3	6.29 \pm 0.23	6.48 \pm 0.18	6.46 \pm 0.16	6.72 \pm 0.16	6.76 \pm 0.17
17	E 301	5,442.8	46.9 \pm 1.9	45.9 \pm 1.5	45.77 \pm 1.2	45.5 \pm 1.0	45.8 \pm 0.67
18	E 305	2,702.4	13.7 \pm 0.55	13.1 \pm 0.42	13.3 \pm 0.36	13.4 \pm 0.35	13.6 \pm 0.32
	$\sum_{i=1}^{18} m$		340.8 g 93%	356.8 g 97%	361.8 g 98%	359.6 g 98%	368.3 g 100%
	$\sum_{i=3}^{18} m$		250.0 g 96%	254.5 g 98%	258.6 g 99%	259.9 g 100%	260.6 g 100%

TABLE 5 - VDC-Results

Run No.	Sample Code	C _o (cps)	Pu-240 Equivalent (g)			
			τ_1	τ_2	τ_3	τ_4
1	E-151	3484.98	24.98 ± 0.76	25.13 ± 0.58	25.92 ± 0.49	26.16 ± 0.46
2	E-243-2	3398.1	6.69 ± 0.62	6.82 ± 0.45	6.69 ± 0.37	6.84 ± 0.36
3	E-246	2465.5	3.96 ± 0.37	4.06 ± 0.27	3.87 ± 0.23	4.24 ± 0.23
4	E-247-2	815.7	2.71 ± 0.09	2.65 ± 0.07	2.63 ± 0.06	2.60 ± 0.07
5	E-250	21920.0	35.96 ± 16.4	43.52 ± 10.6	43.26 ± 8.1	44.26 ± 6.91
6	E-272-1	472.5	2.91 ± 0.06	2.88 ± 0.05	2.87 ± 0.04	2.82 ± 0.04
7	E-272-3	202.4	1.38 ± 0.03	1.37 ± 0.02	1.35 ± 0.02	1.32 ± 0.02
8	E-275-1	469.8	2.69 ± 0.06	2.77 ± 0.04	2.75 ± 0.04	2.65 ± 0.04
9	E-275-2	14438.2	18.06 ± 7.8	21.49 ± 5.3	20.31 ± 4.1	22.11 ± 3.5
10	E-277-2	4363.0	9.60 ± 0.93	9.95 ± 0.67	10.18 ± 0.55	10.13 ± 0.51
11	E-281-1	15031.9	47.79 ± 7.64	50.85 ± 5.2	51.1 ± 3.9	50.35 ± 3.4
12	E-281-2	8979.9	34.59 ± 3.21	36.60 ± 2.3	36.1 ± 1.8	36.27 ± 1.5
13	E-283	12813.6	29.9 ± 6.2	33.7 ± 4.2	32.7 ± 3.3	30.82 ± 2.9
14	E-283-3	5136.5	15.5 ± 1.3	15.6 ± 0.91	15.8 ± 0.73	15.7 ± 0.67
15	E-284-1	2135.5	8.62 ± 0.33	8.85 ± 0.25	9.10 ± 0.22	9.13 ± 0.20
16	E-284-2	860.7	3.15 ± 0.10	3.17 ± 0.08	3.27 ± 0.08	3.27 ± 0.07
17	E-151	3513.5	24.9 ± 0.7	25.4 ± 0.58	26.0 ± 0.49	26.3 ± 0.45

Table 5 - contd.

18	E-243-2	3409.7	6.29 ± 0.62	6.63 ± 0.45	6.71 ± 0.37	6.76 ± 0.36
19	E-246	2465.1	3.89 ± 0.37	3.94 ± 0.27	3.96 ± 0.23	4.41 ± 0.23
20	E-247-2	824.5	2.56 ± 0.09	2.59 ± 0.075	2.60 ± 0.07	2.56 ± 0.07
21	E-250	21677.7	46.2 ± 15.2	48.0 ± 10.2	46.6 ± 7.81	50.5 ± 6.54
22	E-272-1	474.6	2.83 ± 0.06	2.84 ± 0.05	2.82 ± 0.04	2.83 ± 0.04
23	E-272-3	202.3	1.37 ± 0.03	1.34 ± 0.02	1.32 ± 0.02	1.32 ± 0.02
24	E-275-1	472.6	2.84 ± 0.06	2.72 ± 0.04	2.73 ± 0.04	2.70 ± 0.04
25	E-275-2	14438.3	15.0 ± 7.3	18.9 ± 5.3	21.8 ± 4.1	17.9 ± 3.6
26	E-277-2	4389.8	10.3 ± 0.95	10.2 ± 0.68	10.3 ± 0.56	10.4 ± 0.52
27	E-281-1	15061.8	52.9 ± 7.4	53.2 ± 5.2	53.0 ± 3.9	52.6 ± 3.4
28	E-281-2	9041.3	34.6 ± 3.2	35.4 ± 2.3	35.6 ± 1.8	35.8 ± 1.6
29	E-283	12866.0	29.5 ± 6.2	32.3 ± 4.3	32.6 ± 3.3	32.6 ± 2.9
30	E-284-1	2121.3	8.51 ± 0.32	8.51 ± 0.25	8.51 ± 0.21	8.77 ± 0.02
31	E-284-2	871.4	3.32 ± 0.10	3.23 ± 0.08	3.26 ± 0.07	3.31 ± 0.07
32	E-283-3	5191.5	15.2 ± 1.0	15.8 ± 0.92	16.1 ± 0.75	16.2 ± 0.68
33	E-274-1	574.4	2.66 ± 0.07	2.60 ± 0.05	2.60 ± 0.05	2.69 ± 0.68
34	E-130	394.3	2.33 ± 0.05	2.21 ± 0.04	2.20 ± 0.03	2.22 ± 0.03
35	E-255-2	2557.8	7.38 ± 0.41	7.25 ± 0.30	7.22 ± 0.26	7.15 ± 0.25
36	F-274-2	7628.1	13.1 ± 2.4	13.8 ± 1.7	13.9 ± 1.3	14.1 ± 1.2
37	E-277 ^a	2257.3	5.41 ± 0.33	5.49 ± 0.25	5.40 ± 0.21	5.33 ± 0.21
38	E-269-1	4978.2	29.6 ± 1.24	30.0 ± 0.92	30.4 ± 0.76	30.4 ± 0.68
39	E-199-1	322.1	1.98 ± 0.04	1.96 ± 0.03	1.97 ± 0.03	1.96 ± 0.03
40	E-277-1	846.8	1.82 ± 0.09	1.82 ± 0.07	1.82 ± 0.06	1.82 ± 0.07

Table 5 - contd.

41	E-279	700.2	2.19 ± 0.07	2.15 ± 0.06	2.13 ± 0.05	2.05 ± 0.05
42	E-208-2	897.9	3.64 ± 0.10	3.67 ± 0.08	3.71 ± 0.07	3.64 ± 0.08
43	E-282	758.9	1.42 ± 0.08	1.41 ± 0.06	1.40 ± 0.05	1.45 ± 0.06
44	E-120	585.5	3.50 ± 0.07	3.44 ± 0.06	3.48 ± 0.05	3.51 ± 0.05
45	E-252	8239.4	19.6 ± 2.8	19.7 ± 1.9	20.4 ± 1.5	19.8 ± 1.3
46	E-244-2	3359.6	11.5 ± 0.64	11.5 ± 0.47	11.6 ± 0.39	11.6 ± 0.37
47	E-177	491.8	3.16 ± 0.06	3.14 ± 0.05	3.10 ± 0.04	3.06 ± 0.04
48	E-209	265.8	1.30 ± 0.03	1.28 ± 0.02	1.30 ± 0.02	1.31 ± 0.02
49	E-178	265.7	1.41 ± 0.03	1.35 ± 0.02	1.35 ± 0.02	1.34 ± 0.02
50	E-283-2	3163.5	6.98 ± 0.56	7.22 ± 0.41	7.55 ± 0.34	7.29 ± 0.33
51	E-226	1045.9	5.88 ± 0.13	5.88 ± 0.10	5.80 ± 0.09	5.76 ± 0.09
52	E-245	4809.9	17.7 ± 1.2	13.1 ± 0.84	18.3 ± 0.68	18.6 ± 0.62
53	E-272-2	21863.9	50.5 ± 15.0	52.7 ± 10	52.7 ± 7.61	54.0 ± 6.5
54	E-137	942.7	5.23 ± 0.12	5.35 ± 0.09	5.26 ± 0.08	5.31 ± 0.08
55	E-156	921.9	5.22 ± 0.12	5.31 ± 0.09	5.32 ± 0.08	5.19 ± 0.08
56	E-282 ^b	218.5	1.21 ± 0.03	1.18 ± 0.02	1.16 ± 0.02	1.18 ± 0.02
57	E-183-2	6609.3	29.6 ± 1.96	30.0 ± 1.41	29.6 ± 1.13	29.8 ± 1.00
58	E-275	275.8	1.62 ± 0.04	1.61 ± 0.03	1.61 ± 0.02	1.58 ± 0.02
59	E-174	1436.5	6.72 ± 0.19	6.69 ± 0.15	6.78 ± 0.13	6.73 ± 0.01
60	E-243-3	12868.5	15.9 ± 6.35	17.2 ± 4.3	19.7 ± 3.3	19.3 ± 2.9
61	E-248	2777.1	6.07 ± 0.45	6.56 ± 0.34	6.46 ± 0.28	6.71 ± 0.28
62	E-202	1122.3	1.88 ± 0.12	1.82 ± 0.09	1.82 ± 0.08	1.83 ± 0.09
63	E-286-1	3286.9	7.70 ± 0.59	8.10 ± 0.43	7.97 ± 0.36	8.11 ± 0.35

Table 5 - contd.

64	E-244-3	1927.4	5.67 ± 0.27	7.93 ± 0.22	9.64 ± 0.20	9.42 ± 0.19
65	E-131-3	138.9	0.45 ± 0.02	0.45 ± 0.01	0.45 ± 0.01	0.42 ± 0.01
66	E-244-1	1368.04	5.25 ± 0.18	5.45 ± 0.14	5.41 ± 0.12	5.49 ± 0.12
67	E-146-1	515.7	3.23 ± 0.06	3.15 ± 0.05	3.13 ± 0.05	3.17 ± 0.05
68	E-208-1	1810.4	10.1 ± 0.27	10.3 ± 0.21	10.4 ± 0.19	10.6 ± 0.18
69	E-278	5508.4	8.66 ± 1.39	8.88 ± 0.97	9.03 ± 0.78	8.72 ± 0.72
70	E-215	530.3	2.07 ± 0.06	2.03 ± 0.04	2.02 ± 0.04	2.04 ± 0.04
71	E-191-2	3593.3	24.8 ± 0.79	24.5 ± 0.60	24.3 ± 0.50	24.0 ± 0.46
72	E-270	1318.2	3.76 ± 0.16	3.52 ± 0.12	3.60 ± 0.11	3.55 ± 0.11
73	E-152-2*	134.3	0.157 ± 0.014	0.162 ± 0.011	0.100 ± 0.01	0.170 ± 0.01
74	E-276	238.6	1.39 ± 0.03	1.38 ± 0.02	1.37 ± 0.02	1.35 ± 0.02
75	E-247	1147.3	3.78 ± 0.14	3.77 ± 0.10	3.73 ± 0.09	3.77 ± 0.10
76	E-101	1084.7	2.40 ± 0.12	2.36 ± 0.03	2.35 ± 0.08	2.41 ± 0.09
77	E-271-2	1380.0	8.85 ± 0.20	8.72 ± 0.15	8.70 ± 0.13	8.60 ± 0.13
78	E-249	1179.4	2.58 ± 0.13	2.56 ± 0.10	2.53 ± 0.09	2.50 ± 0.09
79	E-207	550.5	3.23 ± 0.07	3.21 ± 0.05	3.17 ± 0.05	3.11 ± 0.05
80	E-146-2	2190.4	14.4 ± 0.37	14.6 ± 0.29	14.7 ± 0.25	14.7 ± 0.24
81	E-123	706.9	4.35 ± 0.09	4.3 ± 0.07	4.32 ± 0.06	4.34 ± 0.06
82	E-119	602.5	3.19 ± 0.07	3.26 ± 0.06	3.26 ± 0.05	3.15 ± 0.05
83	E-247-3	2517.3	6.15 ± 0.39	6.37 ± 0.29	6.27 ± 0.25	5.91 ± 0.24
84	E-243-1	442.7	2.42 ± 0.05	2.51 ± 0.04	2.45 ± 0.04	2.50 ± 0.04
85	E-100	415.1	2.61 ± 0.05	2.60 ± 0.04	2.60 ± 0.04	2.60 ± 0.04
86	E-285*	15.5	0.079 ± 0.006	0.081 ± 0.005	0.080 ± 0.004	0.083 ± 0.004

Table 5 - contd.

87	E-131*	28.8	0.166± 0.010	0.167± 0.008	0.170± 0.007	0.168± 0.006
88	E-275*	53.6	0.086± 0.008	0.091± 0.006	0.091± 0.006	0.093± 0.006
89	E-279*	28.5	0.082± 0.007	0.141± 0.007	0.144± 0.006	0.139± 0.006
90	E-276*	35.5	0.215± 0.011	0.208± 0.009	0.208± 0.007	0.211± 0.007
91	E-278*	34.1	0.172± 0.010	0.159± 0.008	0.157± 0.006	0.157± 0.006
92	E-284*	6.25	0.032± 0.004	0.030± 0.003	0.033± 0.002	0.032± 0.002
93	E-270*	5.74	0.021± 0.003	0.023± 0.002	0.027± 0.002	0.026± 0.002
94	E-200	1359.0	8.23 ± 0.24	8.16 ± 0.18	8.37 ± 0.16	8.44 ± 0.17
95	E-301	5360.7	44.2 ± 1.6	43.7 ± 1.2	43.5 ± 0.99	43.7 ± 0.88
96	E-302	159.9	0.830± 0.03	0.82 ± 0.02	0.81 ± 0.02	0.80 ± 0.02
97	E-303	830.1	4.66 ± 0.13	4.77 ± 0.11	4.64 ± 0.09	4.55 ± 0.10
98	E-304	927.7	4.52 ± 0.15	4.47 ± 0.11	4.35 ± 0.10	4.57 ± 0.11
99	E-305	2657.7	14.10 ± 0.55	14.13 ± 0.42	13.9 ± 0.36	13.9 ± 0.35
100	E-306	767.2	4.10 ± 0.12	4.17 ± 0.10	4.19 ± 0.09	4.18 ± 0.09
101	E-307	445.1	5.43 ± 0.14	5.28 ± 0.11	5.24 ± 0.10	5.18 ± 0.10
102	E-308	1875.9	10.67 ± 0.35	10.79 ± 0.27	10.72 ± 0.24	10.39 ± 0.24
103	E-250	22039.1	33.67 ± 16.8	41.70 ± 10.9	45.14 ± 8.1	43.82 ± 7.0
104	E-208-1	1826.8	10.16 ± 0.30	10.37 ± 0.26	10.42 ± 0.23	10.76 ± 0.23
105	E-271-2	1402.2	8.69 ± 0.25	8.74 ± 0.19	9.02 ± 0.17	9.31 ± 0.18
106	E-255-2	2611.6	7.59 ± 0.50	7.78 ± 0.37	7.49 ± 0.82	7.35 ± 0.32
107	E-269-1	4926.2	31.39 ± 1.38	31.19 ± 1.03	31.34 ± 0.86	30.52 ± 0.79
108	E-281-2	8702.0	35.62 ± 3.22	36.92 ± 2.30	36.82 ± 1.82	38.17 ± 1.59
109	E-137	943.4	5.34 ± 0.15	5.31 ± 0.12	5.30 ± 0.11	5.33 ± 0.11

Table 5 - contd.

110	E-183-2	6619.3	30.03 ± 2.1	31.1 ± 1.5	30.7 ± 1.2	29.8 ± 1.1
111	E-174	1439.6	6.87 ± 0.24	6.81 ± 0.19	7.05 ± 0.17	6.97 ± 0.17
112	E-272-2	22346.5	49.13 ± 15.8	52.7 ± 10.4	54.8 ± 7.8	48.4 ± 6.9
113	E-244-3	1948.7	9.79 ± 0.36	9.70 ± 0.28	9.92 ± 0.24	10.07 ± 0.24
114	E-243-3	12947.3	17.06 ± 6.4	18.8 ± 4.4	19.5 ± 3.4	20.9 ± 2.9
115	E-283-2	3176.1	7.37 ± 0.65	7.24 ± 0.48	6.99 ± 0.40	6.65 ± 0.39
116	E-245	4845.5	19.1 ± 1.2	23.4 ± 0.97	18.2 ± 0.78	18.8 ± 0.72
117	E-250	22100.5	44.9 ± 15.9	48.8 ± 10.5	49.0 ± 7.9	51.6 ± 6.7
118	E-272-2	22401.8	44.5 ± 16.3	50.0 ± 10.7	50.3 ± 8.0	45.0 ± 7.1
119	E-243-3	12944.2	17.8 ± 6.4	20.0 ± 4.4	21.3 ± 3.4	22.5 ± 2.9
120	E-281-2	8720.3	34.4 ± 3.2	34.8 ± 2.3	35.3 ± 1.8	36.9 ± 1.6
121	E-244-3	1959.3	9.68 ± 0.36	9.78 ± 0.28	9.80 ± 0.24	9.62 ± 0.24
122	E-255-2	2626.4	7.19 ± 0.50	7.36 ± 0.37	7.41 ± 0.32	7.30 ± 0.32
123	E-245	4877.9	17.3 ± 1.3	17.8 ± 0.94	17.7 ± 0.78	17.8 ± 0.72
124	E-283-2	3143.1	7.63 ± 0.64	7.20 ± 0.47	7.84 ± 0.40	7.68 ± 0.39
125	E-137	948.9	5.26 ± 0.15	5.29 ± 0.12	5.12 ± 0.11	5.19 ± 0.11
126	E-243-2	3425.9	6.13 ± 0.71	6.64 ± 0.52	6.68 ± 0.44	5.83 ± 0.43
127	E-277-2	4374.6	9.60 ± 1.05	9.87 ± 0.76	9.92 ± 0.63	9.98 ± 0.60
128	E-183-2	6670.2	29.0 ± 2.1	28.8 ± 1.5	30.1 ± 1.25	28.7 ± 1.1
129	E-271-2	1399.3	8.73 ± 0.25	8.76 ± 0.19	9.00 ± 0.17	9.16 ± 0.17
130	E-208-1	1819.1	10.2 ± 0.33	10.4 ± 0.26	10.6 ± 0.23	10.6 ± 0.23
131	E-269-1	4923.0	29.7 ± 1.37	30.7 ± 1.03	30.6 ± 0.85	30.2 ± 0.77
132	E-174	1437.5	6.76 ± 0.24	6.95 ± 0.19	6.91 ± 0.17	7.16 ± 0.17

Table 5 - contd.

133	E-301	5442.7	46.0 ± 1.62	45.0 ± 1.22	44.8 ± 1.01	44.6 ± 0.90
134	E-305	2702.4	14.6 ± 0.56	14.4 ± 0.43	14.2 ± 0.37	14.1 ± 0.36

7. FIGURES

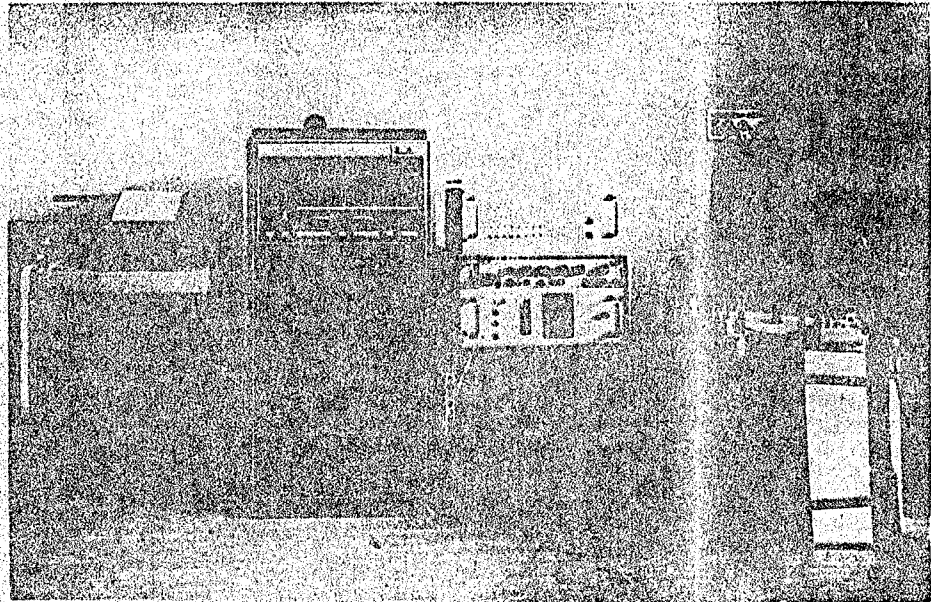


Fig. 1 - GENERAL VIEW OF THE EQUIPMENT

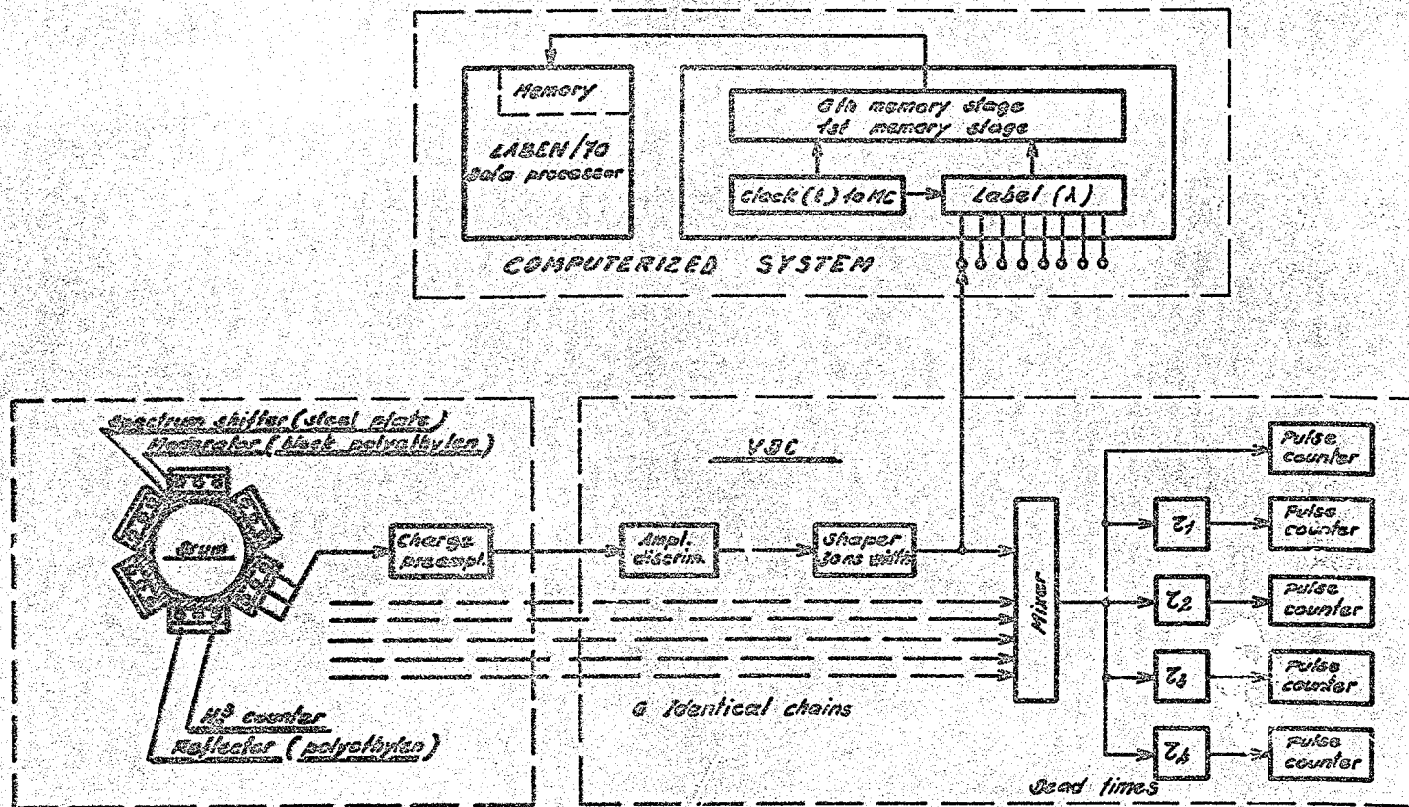


Fig. 2 - Block diagram of Euroform passive neutron assay equipment

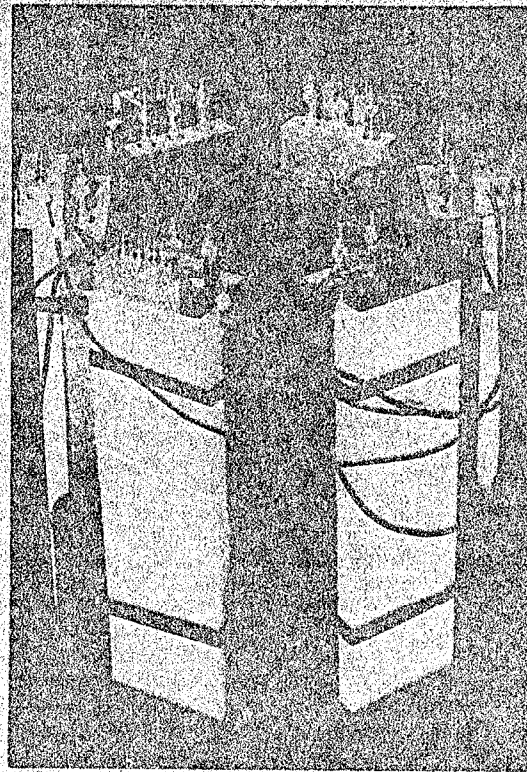
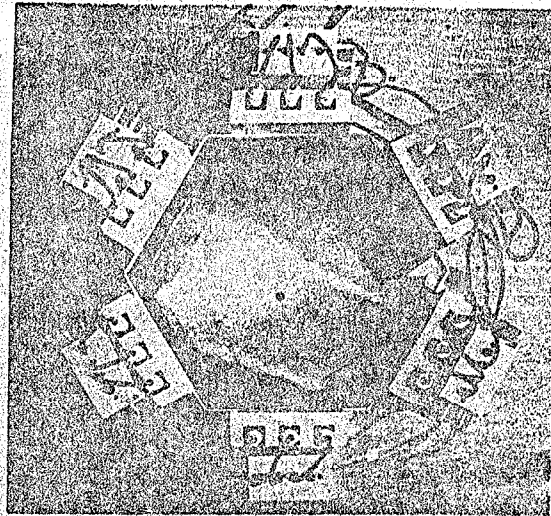


Fig. 3 - TOP AND SIDE VIEWS OF DETECTOR ASSEMBLY

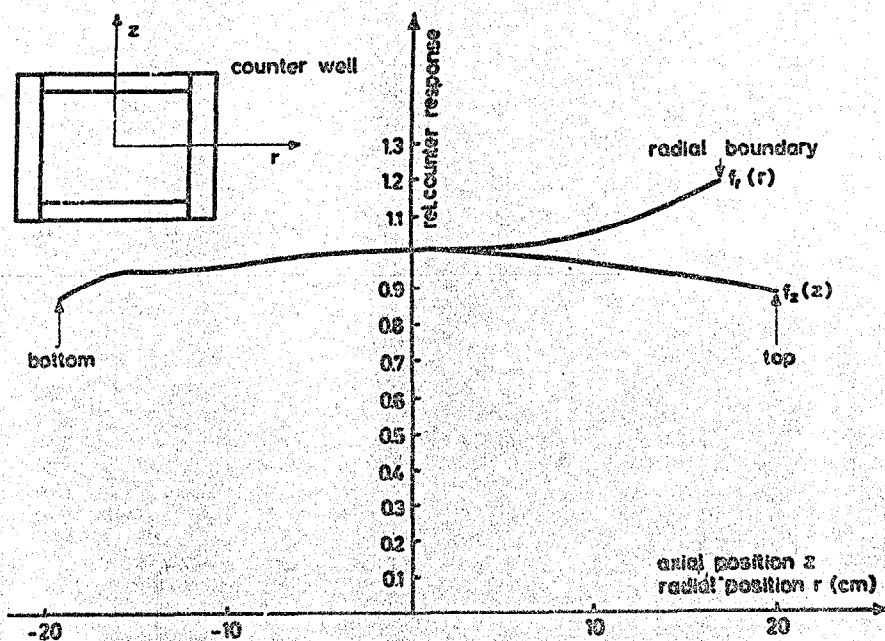


FIG. 4 - AXIAL AND RADIAL COUNTER RESPONSE FUNCTIONS

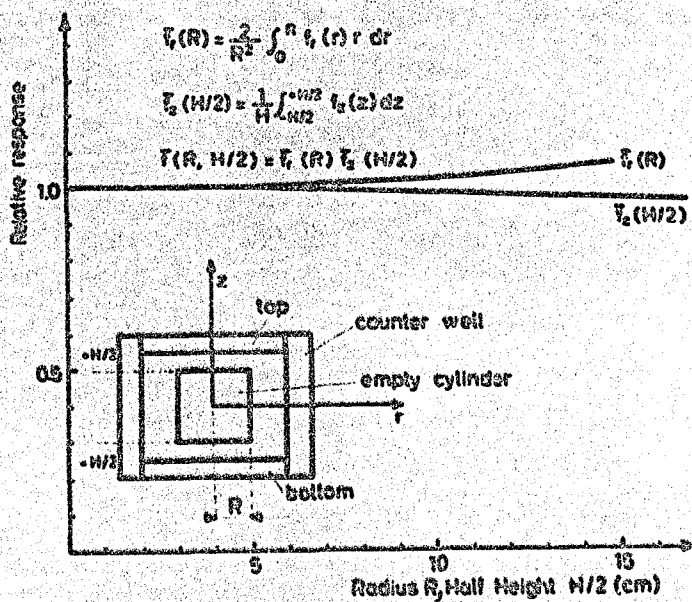


FIG. 5 - COUNTER RESPONSE FUNCTIONS AVERAGED OVER RADIUS R AND HEIGHT H OF EMPTY CYLINDRICAL DRUMS

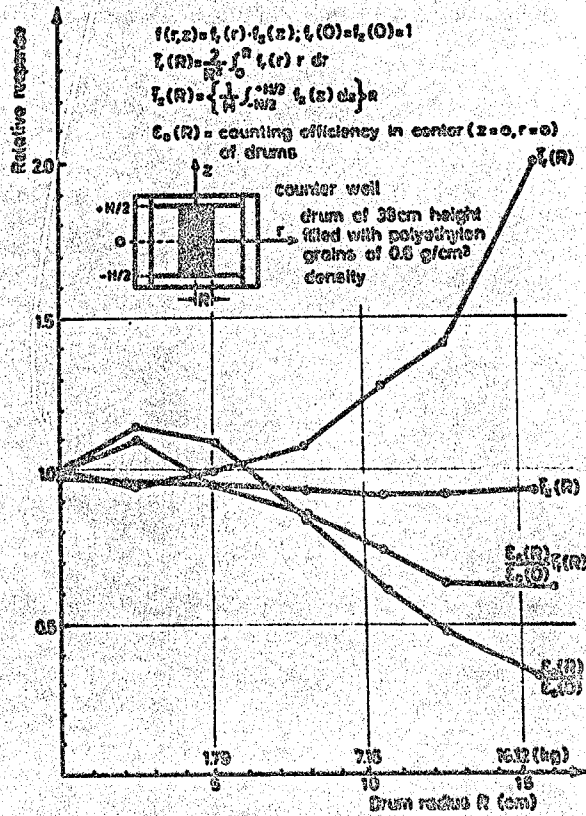


FIG. 6-MODERATING MATRIX EFFECT ON COUNTER RESPONSE FUNCTIONS

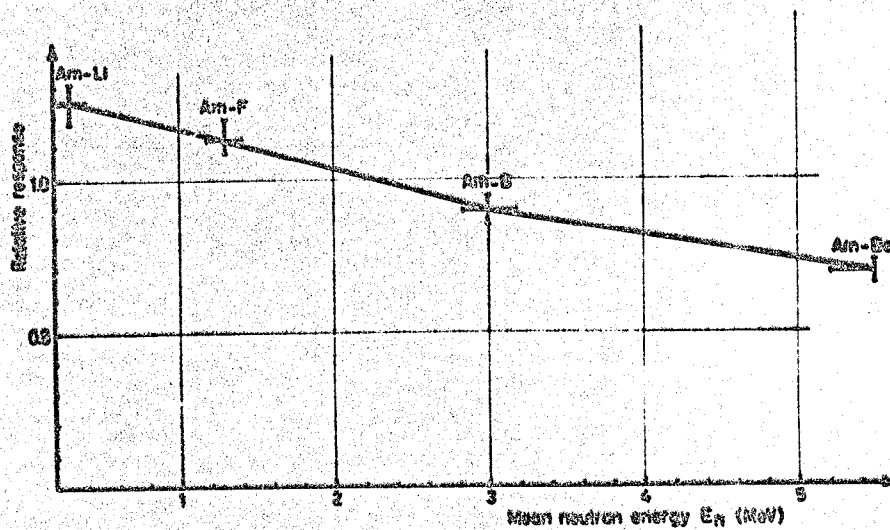


FIG. 7-COUNTER RESPONSE AS A FUNCTION OF NEUTRON ENERGY

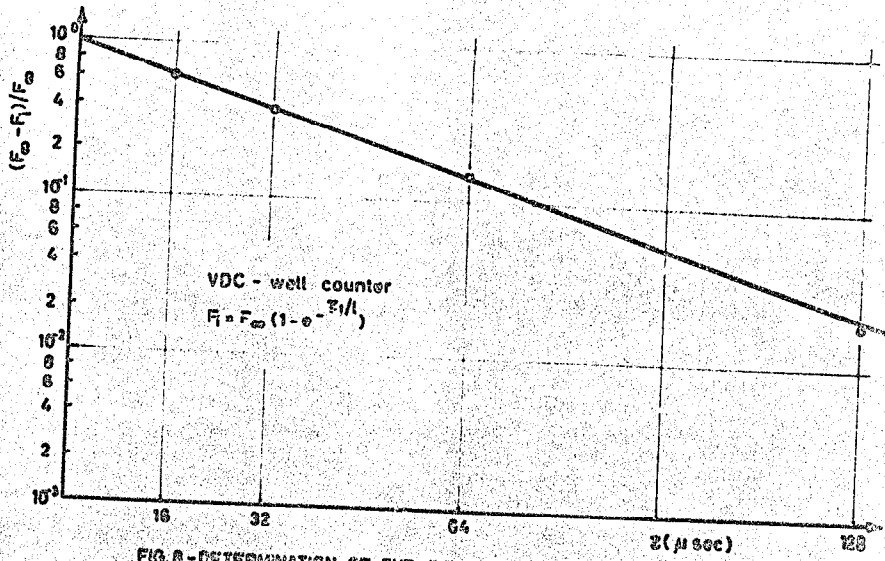


FIG. 6 - DETERMINATION OF THE DECAY TIME BY VDC

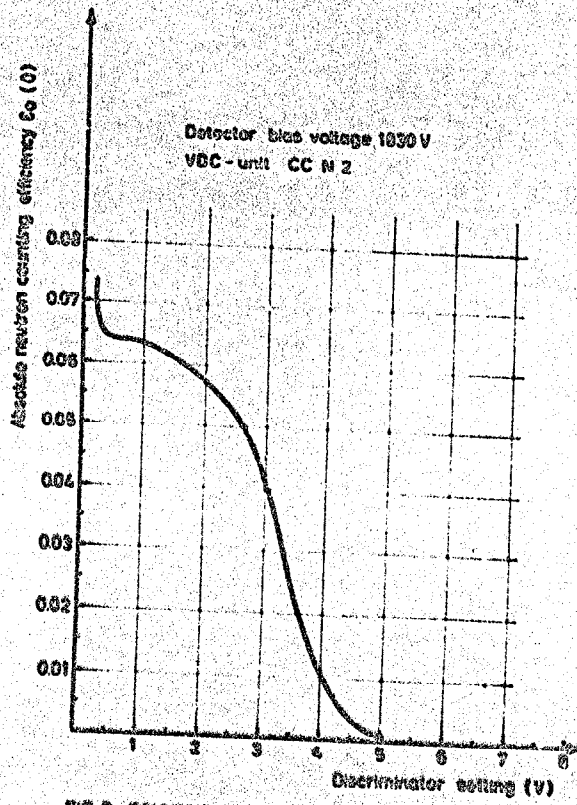


FIG. 5 - COUNTING EFFICIENCY AS A FUNCTION OF DISCRIMINATOR SETTING

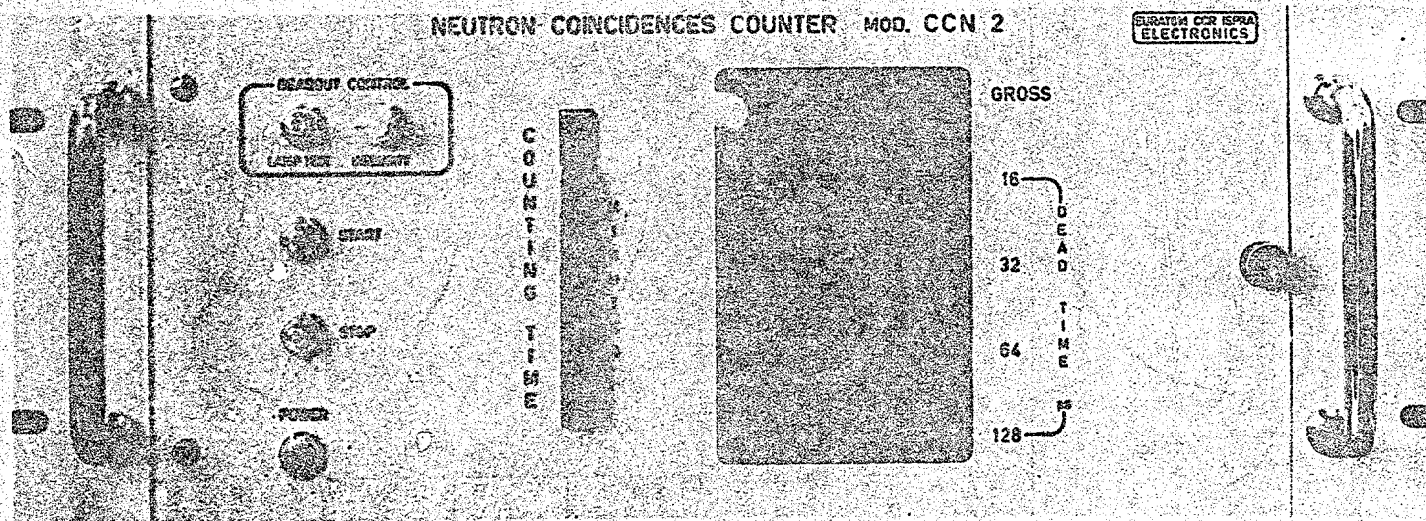


Fig. 10 - THE VARIABLE DEAD TIME (VDC) - COUNTER

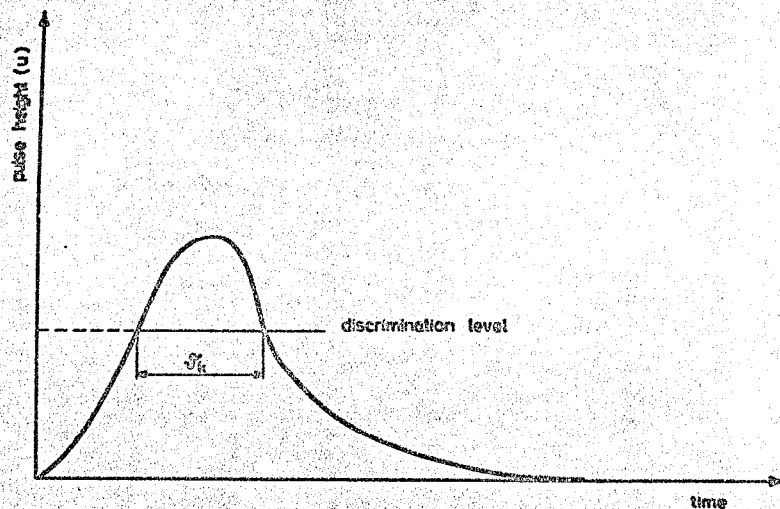


FIG. 11 - EXPLANATION OF THE DISCRIMINATOR PARALYSIS TIME σ_A

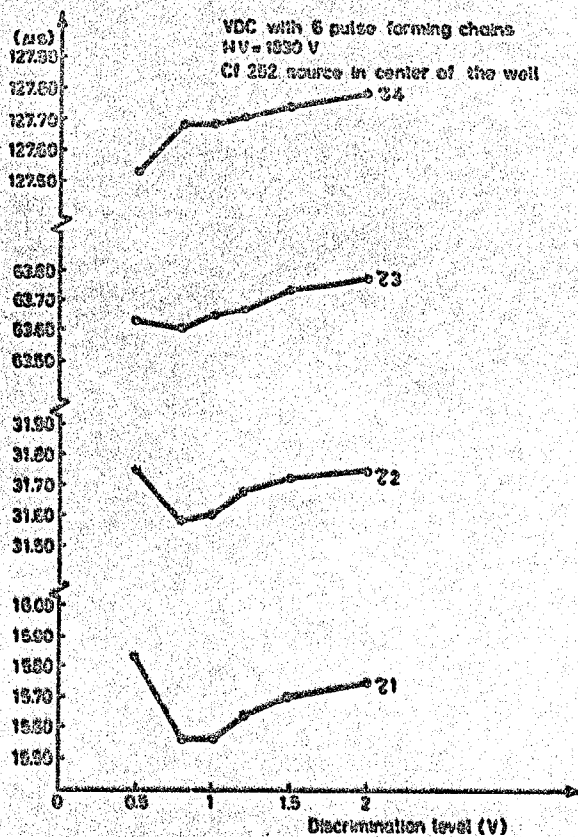


FIG. 12 - COUNTER DEAD TIMES AS FUNCTIONS OF DISCRIMINATION LEVEL

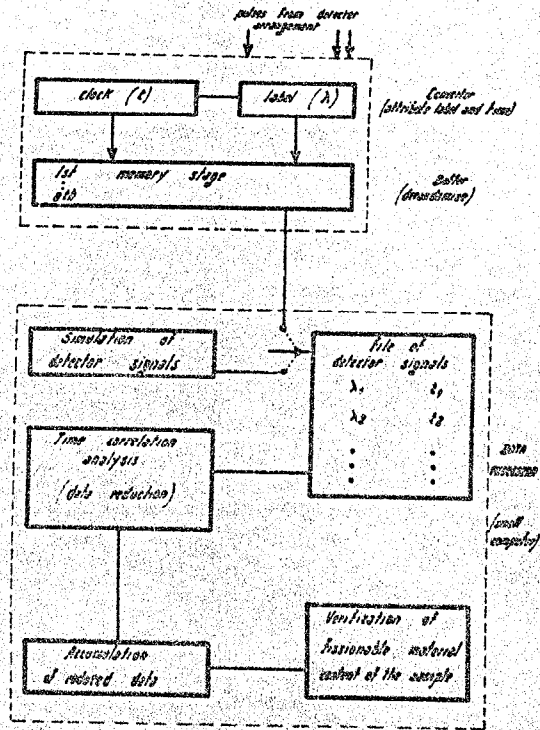


Fig. 15. Computerized system for time correlation analysis of nuclear evolution rates - (schematic)

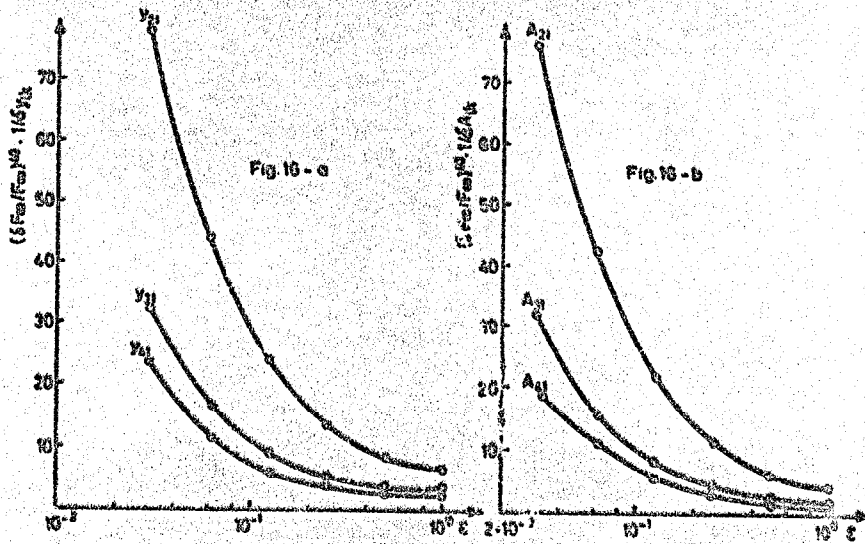


FIG 16-RELATIVE UNCERTAINTY OF F_{00} DETERMINATION AS A FUNCTION OF COUNTING EFFICIENCY ϵ

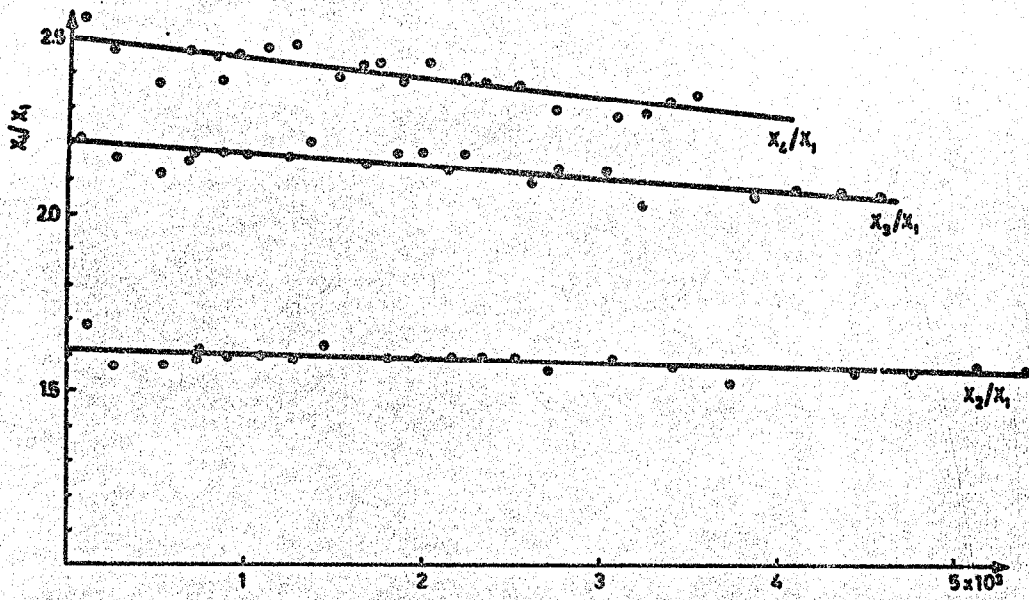


FIG. 17-LINEAR VARIATION OF X_i/X_1 ($i=2,3,4$) AS A FUNCTION OF COUNT RATE C_i

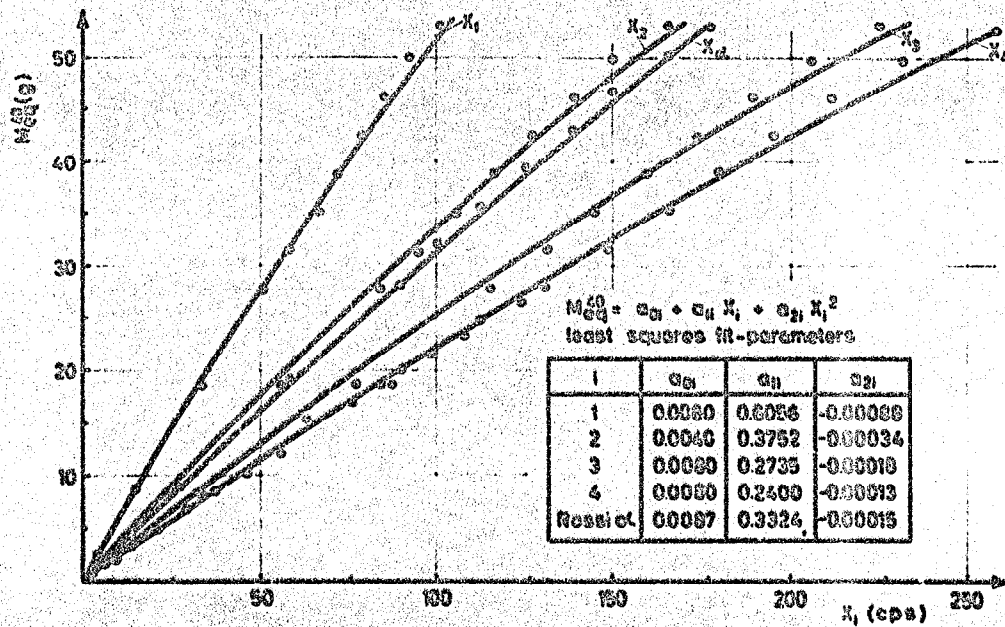
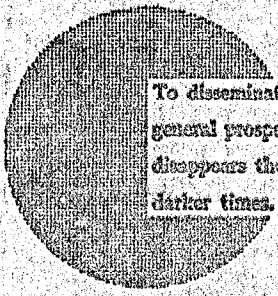


Fig.18-CALIBRATION CURVES-VDC (X_1) ROSSI α (NaI)

NOTICE TO THE READER

All scientific and technical reports published by the Commission of the European Communities are announced in the monthly periodical "euro-abstracts". For subscription (1 year: B.Fr. 1 025,—) or free specimen copies please write to:

Office for Official Publications
of the European Communities
Boite postale 1033
Luxembourg
(Grand-Duchy of Luxembourg)



To disseminate knowledge is to disseminate prosperity — I mean general prosperity and not individual riches — and with prosperity disappears the greater part of the evil which is our heritage from darker times.

Alfred Nobel